

**Complete set of first-order polarization observables
in nucleon-deuteron elastic scattering near 20 MeV deuteron energy**

M. Sawada, S. Seki, K. Furuno, Y. Tagishi, Y. Nagashima, J. Schimizu, M. Ishikawa,
T. Sugiyama, L. S. Chuang,* W. Gruebler,[†] and J. Sanada
Tandem Accelerator Center and Institute of Physics, The University of Tsukuba, Ibaraki 305, Japan

Y. Koike and Y. Taniguchi

Department of Nuclear Engineering, Kyoto University, Kyoto 606, Japan

(Received 27 September 1982)

We have measured differential cross section and analyzing powers A_y^p , iT_{11} , T_{20} , T_{21} , and T_{22} for proton-deuteron elastic scattering near 20 MeV deuteron energy. The total error of the differential cross section was 1% or less. Each deuteron analyzing power was measured independently with the maximum efficiency. The total error of the analyzing power was less than 0.007. Faddeev calculations have been performed for three cases of nucleon-nucleon interaction. None of them gives an overall quantitative fit to the measured values. The effect of the Coulomb interaction is discussed.

$$\left[\begin{array}{l} \text{NUCLEAR REACTIONS } ^2\text{H}(\vec{p}, p)^2\text{H}, E_p = 11.1 \text{ MeV; measured } \sigma_0(\theta), \\ A_y^p(\theta); ^1\text{H}(\vec{d}, d)^1\text{H}, E_d = 17.0, 20.0, 22.2 \text{ MeV; measured } iT_{11}(\theta), T_{20}(\theta), \\ T_{21}(\theta), T_{22}(\theta). \text{ Faddeev calculations.} \end{array} \right]$$

I. INTRODUCTION

In the 1960's a theoretical method to investigate details of the nucleon-nucleon interactions through the study of three-nucleon scattering was developed by Amado, Lovelace, and Alt *et al.*,¹ starting from Faddeev theory. The nucleon-deuteron scattering process has been investigated extensively both experimentally and theoretically during the last decade, and the need for very accurate measurements on a complete set of the zeroth and first order observables for spin variables, especially tensor analyzing powers, has been recognized in order to test the highly sophisticated theoretical predictions around $E_d^{\text{lab}} = 20 \text{ MeV}$.²

For such measurements, a precise absolute value of the polarization of deuteron beams is essential, and it is obvious that the use of a Lamb-shift type of polarized ion source with a spin filter joined to a tandem accelerator is the most suitable way to obtain it.

Here we report the results of measurements and Faddeev calculations, and comparisons between them. The measured quantities are $\sigma_0(\theta)$ and $A_y^p(\theta)$ at $E_p^{\text{lab}} = 11.1 \text{ MeV}$; $iT_{11}(\theta)$ at $E_d^{\text{lab}} = 20.0$ and 22.2 MeV ; $T_{21}(\theta)$ at $E_d^{\text{lab}} = 17.0, 20.0,$ and 22.2 MeV ; and $T_{20}(\theta)$ and $T_{22}(\theta)$ at $E_d^{\text{lab}} = 22.2 \text{ MeV}$ in proton-deuteron elastic scattering. Faddeev calculations are

for $\sigma_0(\theta)$ and $A_y^p(\theta)$ at $E_p^{\text{lab}} = 11.1 \text{ MeV}$; and $iT_{11}(\theta)$, $T_{20}(\theta)$, $T_{21}(\theta)$, and $T_{22}(\theta)$ at $E_d^{\text{lab}} = 22.2 \text{ MeV}$.

Some experimental results were presented at the Few Nucleon Conference at Graz³ and the Polarization Phenomena Symposium at Santa Fe.⁴

II. EXPERIMENTAL PROCEDURES

Polarized proton and deuteron beams were produced by use of a Lamb-shift type of polarized ion source with a spin filter and a spin precessor magnet.⁵ Beams were accelerated through a 12 UD Pelletron tandem accelerator⁶ and focused on the target through a beam-transport system. The target material was hydrogen or deuterium gas in a small gas cell with a $2.5 \mu\text{m}$ thick Havar window which was installed at the center of a large general purpose scattering chamber.

Scattered particles were detected by four counter telescopes composed of a thin silicon surface-barrier detector and a thick one, installed so that there were two on the left turntable and two on the right turntable. Particle identifiers were used if we had a need to separate the particles.

The differential cross section was measured independently of the analyzing-power measurements. Estimated typical errors and their sources considered were as follows: 0.47% for counting statis-

tics, 0.06% for angle setting, 0.12% for current integration, 0.50% for the G factor, and 0.23% for the number of scattering centers in the target gas. An overall check for the procedures was made by measuring σ_0 ($\theta_{\text{lab}}=45^\circ$) in proton-proton scattering. The result was 46.4 ± 0.5 mb/sr in the center of mass system, which is compatible with the value of 46.4 ± 0.3 mb/sr obtained through the interpolation of the values at 10 and 14 MeV.

A proton analyzing power $A_y^p(\theta)$ was obtained by measurements with spin-up and spin-down beams and by use of the following formula:

$$A_y^p(\theta) = \frac{I_U(\theta) - I_D(\theta)}{P_U I_U(\theta) + P_D I_D(\theta)}, \quad (1)$$

where P_U and P_D denote degrees of polarization for spin-up and spin-down beams, respectively, and I_U and I_D denote yields with spin-up and spin-down beams, respectively. Namely, four detectors were set at different angles for an efficient measurement. Such a procedure was adopted after we confirmed that the A_y^p reduced by Eq. (1) agrees with the one reduced by the geometric mean method within a fraction of the relevant total error through many runs for proton- ^4He and other scatterings prior to the present work. The degree of polarization of the beam was measured frequently by a quench-ratio method. The accuracy of the quench-ratio method for protons was calibrated by measuring A_y^p in proton- ^4He scattering and comparing this with results of Ohlsen *et al.*⁷ A scale error of the degree of polarization of the proton beams was 2%, including the uncertainty of the direction of the spin quantization axis.

In contrast to the proton analyzing power, the deuteron analyzing powers are more complicated to measure. In the present work, each deuteron analyzing power was obtained independently with the maximum efficiency. The spin substate of the deuteron and the direction of the spin quantization axis on the target for the measurement of each deuteron analyzing power are summarized in Table I. The coordinate system used to describe the scattering and the spin quantization axis is shown in Fig. 1. Deuteron analyzing powers were obtained from the following formulas:

$$iT_{11}(\theta) = \frac{1}{2\sqrt{3}P} \left[\frac{I_p(\theta)}{I_0(\theta)} - \frac{I_p(-\theta)}{I_0(-\theta)} \right], \quad (2)$$

$$T_{20}(\theta) = \frac{1}{\sqrt{2}P} \left[1 - \frac{I_p(\theta)}{I_0(\theta)} \right], \quad (3)$$

$$T_{21}(\theta) = \frac{1}{2\sqrt{3}P} \left[\frac{I_p(-\theta)}{I_0(-\theta)} - \frac{I_p(\theta)}{I_0(\theta)} \right], \quad (4)$$

TABLE I. Spin substate and spin quantization axis.

Observables	Spin substate	Spin axis
iT_{11}	$m_I=1$	$\theta_s=90^\circ, \phi_s=90^\circ$
T_{20}	$m_I=0$	$\theta_s=0$
T_{21}	$m_I=0$	$\theta_s=45^\circ, \phi_s=180^\circ$
T_{22}	$m_I=0$	$\theta_s=90^\circ, \phi_s=90^\circ$ for P_1
		$\theta_s=90^\circ, \phi_s=0^\circ$ for P_2

and

$$T_{22}(\theta) = \frac{1}{2\sqrt{3}} \left\{ \left[\frac{I_{p_1}(\theta)}{P_1 I_0(\theta)} - \frac{I_{p_2}(\theta)}{P_2 I_0(\theta)} \right] + \left[\frac{1}{P_2} - \frac{1}{P_1} \right] \right\} - \frac{1}{\sqrt{6}} t_{10} i T_{11}, \quad (5)$$

where P denotes a degree of polarization of the beam, and I_p and I_0 denote yields with polarized and unpolarized beams, respectively. The t_{10} in Eq. (5) denotes a vector polarization of the beam for the $m_I=0$ substate, and amounts to 0.027 in our case. The corresponding P was also corrected by a factor of 0.967, for which we estimated the uncertainty of 1%. The $I_0(\theta)$ in the above equations was determined during the analyzing-power measurements in the pair with the relevant $I_p(\theta)$. The accuracy of

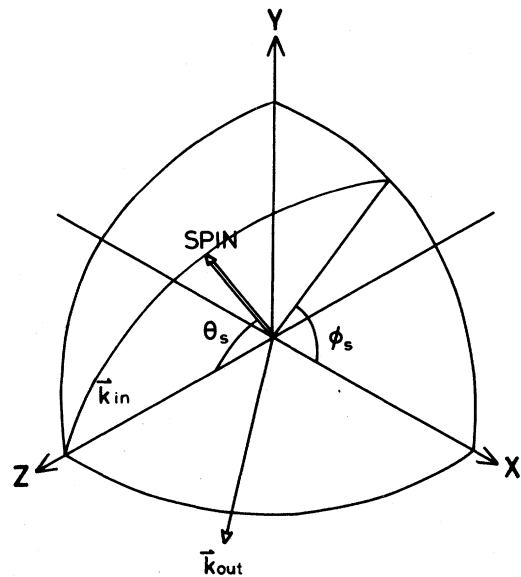


FIG. 1. Coordinate system to define the spin quantization axis.

the quench-ratio method for deuterons was calibrated by measuring the analyzing powers in the $^{16}\text{O}(d,\alpha)^{14}\text{N}^*(2.31\text{ MeV})$ reaction⁸ and deuteron- ^4He elastic scattering.⁹ As a result, a scale error of the degree of polarization of the deuteron beams was 3%, including the uncertainty of the direction of spin quantization axis. The uncertainty of the energies of the beam was 0.2%, and the spread of the energy was 0.4% at the target center.

III. EXPERIMENTAL RESULTS

Experimental results are shown in Figs. 2–7. Circles indicate those at $E_d^{\text{lab}}=11.1\text{ MeV}$ or $E_d^{\text{lab}}=22.2\text{ MeV}$. Squares are of those at $E_d^{\text{lab}}=20.0\text{ MeV}$. Triangles are of those at $E_d^{\text{lab}}=17.0\text{ MeV}$. Error bars indicate absolute errors which are mainly due to the scale error and the counting statistics, the latter being less than 0.006.

The agreement between the present data on $iT_{11}(\theta)$ at $E_d^{\text{lab}}=20.0\text{ MeV}$ and the remeasured data at SIN¹⁰ is quite satisfactory. The data on $T_{21}(\theta)$ at $E_d^{\text{lab}}=17.0$ and 20.0 MeV were taken to supplement the data of Ref. 11 with an aim toward a complete

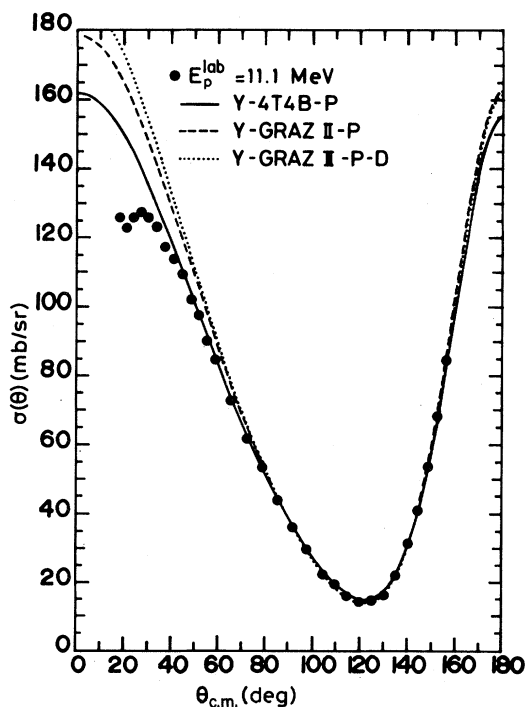


FIG. 2. The differential cross section for nucleon-deuteron elastic scattering. The circles are proton-deuteron experimental results at $E_p^{\text{lab}}=11.1\text{ MeV}$. The lines are neutron-deuteron calculations with different nucleon-nucleon interactions. Full line: *Y-4T4B-P*. Dashed line: *Y-GrazII-P*. Dotted line: *Y-GrazII-P-D*.

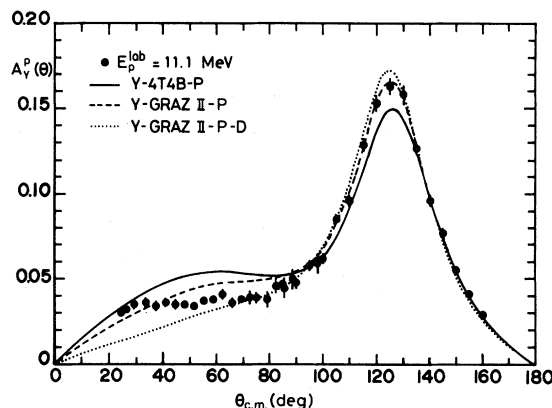


FIG. 3. The nucleon vector analyzing power A_p^p . The circles are proton-deuteron experimental results at $E_p^{\text{lab}}=11.1\text{ MeV}$. The lines are neutron-deuteron calculations. Full line: *Y-4T4B-P*. Dashed line: *Y-GrazII-P*. Dotted line: *Y-GrazII-P-D*.

set for a future energy dependent phase-shift analysis.^{12,13}

For the energy dependence of $T_{21}(\theta)$ near $E_d^{\text{lab}}=20\text{ MeV}$, there existed controversial data and discussion in 1978.^{2,3} This situation is now rectified by the present measurement as seen in Fig. 8, which shows the observed data of $T_{21}(\theta_{\text{c.m.}}=90^\circ)$ from $E_d^{\text{lab}}=10$ to 22 MeV . Closed circles indicate the present results, open circles the data of ETH,¹⁴ and triangles the data of LASL.¹⁵ The magnitude of $T_{21}(\theta_{\text{c.m.}}=90^\circ)$ increases linearly with the increase of incident deuteron energy. Therefore it is interesting to give an empirical excitation function for a future theoretical treatment. The $T_{21}(\theta_{\text{c.m.}}=90^\circ)$ is fitted

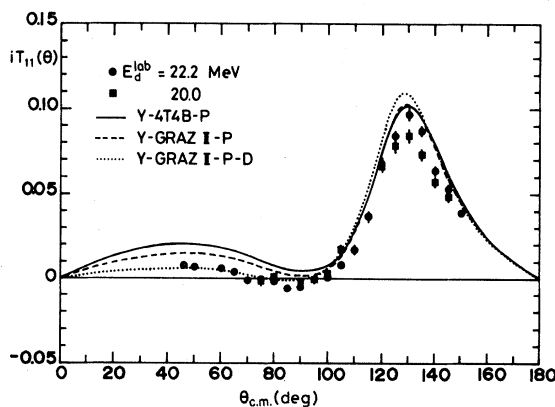


FIG. 4. The deuteron vector analyzing power iT_{11} . The circles are proton-deuteron experimental results at $E_d^{\text{lab}}=22.2\text{ MeV}$. The lines are neutron-deuteron calculations. Full line: *Y-4T4B-P*. Dashed line: *Y-GrazII-P*. Dotted line: *Y-GrazII-P-D*. The squares are proton-deuteron experimental results at $E_d^{\text{lab}}=20.0\text{ MeV}$.

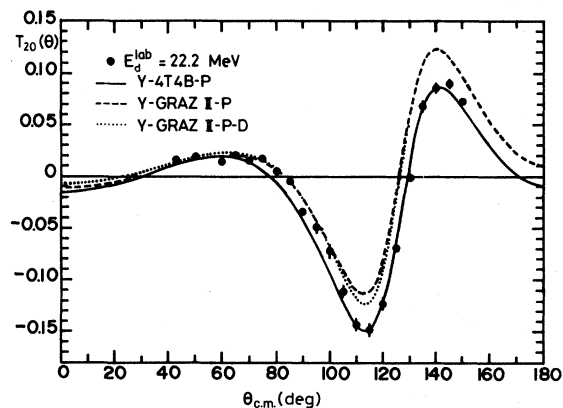


FIG. 5. The tensor analyzing power T_{20} . The circles are proton-deuteron experimental results at $E_d^{\text{lab}}=22.2$ MeV. The lines are neutron-deuteron calculations. Full line: Y-4T4B-P. Dashed line: Y-GrazII-P. Dotted line: Y-GrazII-P-D.

by the relation

$$T_{21}(\theta_{\text{c.m.}}=90^\circ) = -0.0055E_d^{\text{lab}} + 0.0491, \quad (6)$$

where E_d^{lab} is in MeV.

Since it is well known that the maximum value of A_y^p at $\theta_{\text{c.m.}}=125^\circ$ increases linearly from $E_d^{\text{lab}}=4$ to 14 MeV and then reaches a saturated value of about 0.2 above 15 MeV, it is worthwhile to summarize the energy dependence of other deuteron analyzing powers in addition. In the energy range of $E_d^{\text{lab}}=10$ to 22 MeV and for the $\theta_{\text{c.m.}}$ corresponding to a maximum absolute value of each quantity, the following

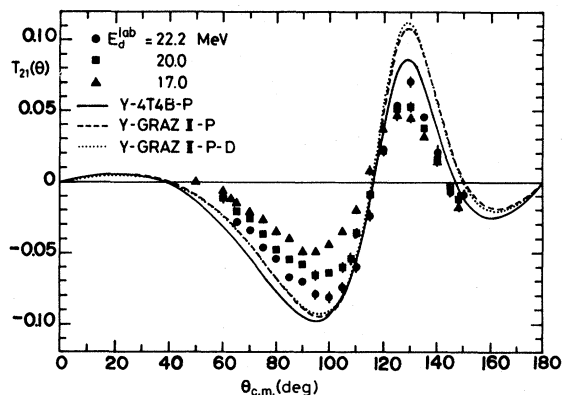


FIG. 6. The tensor analyzing power T_{21} . The circles are proton-deuteron experimental results at $E_d^{\text{lab}}=22.2$ MeV. The lines are neutron-deuteron calculations. Full line: Y-4T4B-P. Dashed line: Y-GrazII-P. Dotted line: Y-GrazII-P-D. The squares and the triangles are proton-deuteron experimental results at $E_d^{\text{lab}}=20.0$ and 17.0 MeV, respectively.

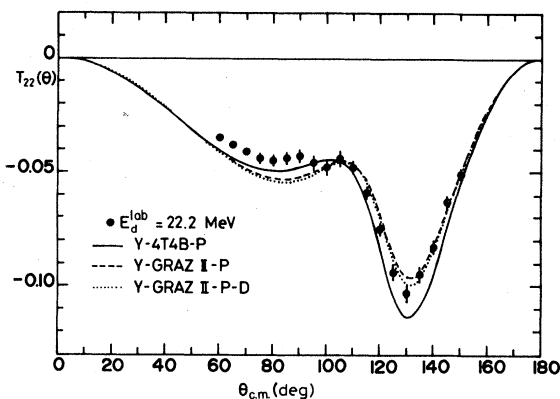


FIG. 7. The tensor analyzing power T_{22} . The circles are proton-deuteron experimental results at $E_d^{\text{lab}}=22.2$ MeV. The lines are neutron-deuteron calculations. Full line: Y-4T4B-P. Dashed line: Y-GrazII-P. Dotted line: Y-GrazII-P-D.

linear relations result:

$$iT_{11}(\theta_{\text{c.m.}}=130^\circ) = 0.0050E_d^{\text{lab}} - 0.0116, \quad (7)$$

$$T_{20}(\theta_{\text{c.m.}}=115^\circ) = -0.014E_d^{\text{lab}} + 0.158, \quad (8)$$

and

$$T_{22}(\theta_{\text{c.m.}}=130^\circ) = -0.0059E_d^{\text{lab}} + 0.0208. \quad (9)$$

The absolute value of the gradient dT_{kq}/dE_d is the largest in T_{20} .

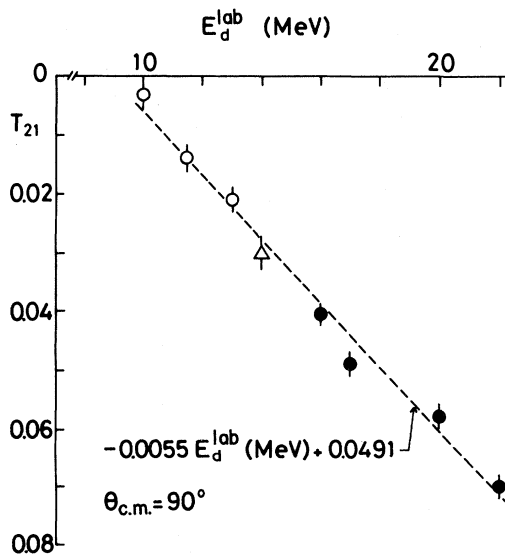


FIG. 8. The excitation curve of the tensor analyzing power at T_{21} at $\theta_{\text{c.m.}}=90^\circ$. The dashed line indicates the fit to the data by a linear function of E_d^{lab} between 10 and 22 MeV.

IV. FADDEEV CALCULATIONS

The first comparisons between experimental data in proton-deuteron elastic scattering and Faddeev calculations in neutron-deuteron elastic scattering for a complete set of observables up to the first order for spin variables were made recently at $E_N^{\text{lab}} = 10$ MeV and $E_d^{\text{lab}} = 20$ MeV.^{10,13} In the calculations, a four-term tensor force with a 4% D -state probability and a repulsive core was adopted in the nucleon-nucleon interaction and denoted by $4T4R$. For the singlet S state, a two-term R -type of form factor was chosen, and denoted by 2^1S_0R . The inclusion of P waves was denoted by $2^1S_0R-4T4R-P$ and the inclusion of P and D waves other than the 3D_1 wave was denoted by $2^1S_0R-4T4R-P-D$. The calculated results agree qualitatively with the experimental data. However, quantitatively, the agreement is poorer in $iT_{11}(\theta)$ and $T_{21}(\theta)$. The inclusion of D waves improves the agreement for the vector analyzing powers at forward angles, and has a negligible effect at backward angles and for other quantities.

Independently, a code for Faddeev calculations was constructed by two (Y.K. and Y.T.) of the authors of this work. The method of solution is different from those of Doleschall¹⁰ and Bruinsma.¹⁶ Preliminary results calculated by this method with the use of simpler interactions between nucleons were reported in Ref. 17.

Further calculations for neutron-deuteron elastic scattering at $E_N^{\text{lab}} = 11.1$ MeV and $E_d^{\text{lab}} = 22.2$ MeV were made in three cases:

In the first calculation, a four term tensor force described in detail in Ref. 18, called $4T4B$, was adopted for 3S_1 and 3D_1 waves. The force $4T4B$ is characterized by a reasonable fit to the mixing parameter ϵ_1 with the empirical values of Ref. 19. For the 1S_0 wave both in neutron-neutron and

neutron-proton interactions the Yamaguchi type of separable potential of Phillips²⁰ was used. For the P waves, we used the P -state nucleon-nucleon interaction of Ref. 18. This first case is denoted by $Y-4T4B-P$. The results are shown by solid lines in Figs. 2–7.

In the second calculation, the neutron-proton interaction for 3S_1 and 3D_1 waves was replaced by the corresponding part of the Graz potential.²¹ It provides an overall realistic description of on- and off-shell properties of the nucleon-nucleon interaction, except for the fit to the mixing parameter ϵ_1 with the empirical values. This second case is denoted by $Y\text{-GrazII-}P$. The results are shown by dashed lines in Figs. 2–7.

To see the contribution of D waves other than 3D_1 waves, the D -state nucleon-nucleon interaction of Ref. 18 was added to the second calculation. This third case is denoted by $Y\text{-GrazII-}P\text{-}D$. The results are shown by dotted lines in Figs. 2–7.

V. DISCUSSION AND CONCLUSION

The difference between $Y\text{-GrazII-}P$ and $Y\text{-GrazII-}P\text{-}D$, namely the effect of the inclusion of D waves other than the 3D wave, is also negligible, except for the vector analyzing powers at forward angles. Therefore we compare the results of Faddeev calculations, which include up to P waves except for 3D_1 waves, with the experimental results. None of the calculations give an overall quantitative fit to measured values.

The partial success of the fit and the extent of the deviation are summarized in Table II. The comparison for the analyzing powers is made at some angles where they have large absolute values.

Calculated vector analyzing powers show the agreement with experimental values within about 10%, which may result from a proper choice of S -

TABLE II. Comparison between experimental and calculated results. "agree" means the calculated value agrees with the measured value within the experimental error. "–7%" denotes that the calculated absolute value is less than the measured one by 7%.

Angular region		$Y-4T4B-P$	$Y\text{-GrazII-}P$	$2^1S_0R-4T4R-P^8$
$\sigma_0(\theta)$		agree at $\theta_{\text{c.m.}} > 40^\circ$	agree at $\theta_{\text{c.m.}} > 80^\circ$	agree at $\theta_{\text{c.m.}} > 60^\circ$
$A_2^p(\theta)$	at $\theta_{\text{c.m.}} = 120^\circ$	–7%	agree	agree
$iT_{11}(\theta)$	at $\theta_{\text{c.m.}} = 130^\circ$	+5%	+5%	+12%
$T_{20}(\theta)$	at $\theta_{\text{c.m.}} = 115^\circ$	agree	–31%	+6%
	at $\theta_{\text{c.m.}} = 140^\circ$	agree	+42%	+5%
$T_{21}(\theta)$	at $\theta_{\text{c.m.}} = 95^\circ$	+23%	+19%	+37%
	at $\theta_{\text{c.m.}} = 130^\circ$	+22%	+53%	+68%
$T_{22}(\theta)$	at $\theta_{\text{c.m.}} = 130^\circ$	+11%	–7%	+4%

and P -state interactions. The agreement or disagreement of calculated values for tensor analyzing powers $T_{2q}(\theta)$ ($q=0,1,2$) with experimental values comes out partly as a consequence of the reasonable or unreasonable fit to the mixing parameter ϵ_1 with the empirical values among the nucleon-nucleon interactions listed in Table II. Above all, this relation is revealed distinctly in the $T_{20}(\theta)$. The $T_{21}(\theta)$ is a quantity which is affected not only by this relation but also by other details of the nucleon-nucleon interaction. The $T_{22}(\theta)$ is insensitive to the things discussed above. The difference of the off-shell property of the nucleon-nucleon interaction is not clear from the present analysis.

Of course, since the experiment was concerned with proton-deuteron scattering, the effect of the Coulomb interaction has to be included. However, we have no rigorous treatment for it. Therefore we calculated an approximate T matrix for the proton-deuteron system by modifying the exact neutron-deuteron T matrix in a manner expressed by Eq. (1) in Ref. 13.

For $\sigma(\theta)$, the improvement of the fit to the data at forward angles (especially at the Coulomb-nuclear interference region) is accompanied unfortunately by departure at backward angles. For vector analyzing powers and $T_{20}(\theta)$, the fit to the existing data is not altered essentially, although a sizable difference in

calculated values between calculations with and without the Coulomb interaction appears at forward angles ($\theta_{c.m.} < 40^\circ$). It is interesting to note that Brock *et al.*²² and Tornow *et al.*²³ point out that the same kind of difference exists between the experimental $A_y^p(\theta)$ in proton-deuteron scattering and neutron-deuteron scattering. For $T_{21}(\theta)$, the improvement of the fit at $\theta_{c.m.} = 130^\circ$ leads at the same time to a departure at $\theta_{c.m.} = 95^\circ$. For $T_{22}(\theta)$, the calculated values are insensitive to the inclusion of the Coulomb interaction in the whole range of the scattering angle.

It appears that a valid conclusion concerning the Coulomb effect cannot be drawn from the procedure described above, although a partial improvement is obtained. Furthermore, we are not yet in a position to discuss the off-shell behavior of the nucleon-nucleon interaction through the study of the first order polarization observables in nucleon-deuteron elastic scattering, much less the possible three-nucleon force.

ACKNOWLEDGMENTS

The authors wish to thank Professor A. Klein for critically reading the manuscript. This work was supported in part by the Nuclear Solid State Research Project at the University of Tsukuba.

*Permanent address: Department of Physics, The Chinese University of Hong Kong, N.T., Hong Kong.

†Permanent address: Laboratorium für Kernphysik, Eidgenössische Technische Hochschule, 8093 Zürich, Switzerland.

¹See, for example, J. S. Levinger, in *Springer Tracts in Modern Physics*, edited by G. Höhler (Springer, New York, 1974), Vol. 71, p. 88.

²W. Grüebler, V. König, P. A. Schmelzbach, B. Jenny, H. Bürgi, P. Doleschall, G. Heidenreich, H. Roser, F. Seiler, and W. Reichart, *Phys. Lett.* **74B**, 173 (1978).

³J. Sanada, S. Seki, Y. Tagishi, W. Grüebler, M. Sawada, Y. Nagashima, K. Furuno, and L. S. Chuang, in *Lecture Notes in Physics 82, Few Body Systems and Nuclear Forces I*, edited by H. Zingl, M. Haftel, and H. Zankel (Springer, Berlin, 1978), p. 246.

⁴M. Sawada, S. Seki, M. Ishikawa, K. Furuno, Y. Nagashima, J. Shimizu, and J. Sanada, in *Polarization Phenomena in Nuclear Physics—1980 (Fifth International Symposium, Santa Fe)*, Proceedings of the Fifth International Symposium on Polarization Phenomena in Nuclear Physics, AIP Conf. Proc. No. 69, edited by G. G. Ohlsen, Ronald E. Brown, Nelson Jarmie, W. W. McNaughton, and G. M. Hale (AIP, New York, 1981), p. 1226.

⁵Y. Tagishi and J. Sanada, *Nucl. Instrum. Methods* **164**, 411 (1979).

⁶S. Seki, K. Furuno, T. Ishihara, Y. Nagashima, M. Yamanouchi, T. Aoki, T. Mikumo, and J. Sanada, *Nucl. Instrum. Methods* **184**, 113 (1981).

⁷G. G. Ohlsen, J. L. McKibben, G. P. Lawrence, P. W. Keaton, Jr., and D. D. Armstrong, *Phys. Rev. Lett.* **27**, 599 (1971).

⁸B. A. Jacobson and R. M. Ryndin, *Nucl. Phys.* **24**, 505 (1961).

⁹G. G. Ohlsen, P. A. Lovoi, G. G. Salzman, U. Meyer-Berkhout, C. K. Mitchell, and W. Grüebler, *Phys. Rev. C* **8**, 1261 (1973).

¹⁰P. Doleschall, W. Grüebler, V. König, P. A. Schmelzbach, F. Sperisen, and B. Jenny, *Nucl. Phys.* **A380**, 72 (1982).

¹¹P. A. Schmelzbach, V. König, W. Grüebler, H. R. Bürgi, B. Jenny, F. Seiler, G. Heidenreich, and H. Roser, see Ref. 3, p. 242.

¹²P. A. Schmelzbach, W. Grüebler, R. E. White, V. König, R. Risler, and P. Marmier, *Nucl. Phys.* **A197**, 273 (1972).

¹³W. Grüebler, *Nucl. Phys.* **A353**, 31c (1981); and private communication.

¹⁴R. E. White, W. Grüebler, V. König, R. Risler, A. Ruh,

- P. A. Schmelzbach, and P. Marmier, Nucl. Phys. A180, 593 (1972); R. E. White, W. Grüebler, B. Jenny, V. König, P. A. Schmelzbach, and H. R. Bürgi, *ibid.* A321, 1 (1979).
- ¹⁵G. G. Ohlsen and P. W. Keaton, private communication.
- ¹⁶J. Bruinsma, thesis, Vrije Universiteit, Amsterdam, 1976.
- ¹⁷Y. Koike, Y. Taniguchi, M. Sawada, and J. Sanada, Prog. Theor. Phys. 66, 1899 (1981).
- ¹⁸F. D. Correll, G. G. Ohlsen, R. E. Brown, R. A. Hardekopf, Nelson Jarmie, and P. Doleschall, Phys. Rev. C 23, 960 (1981).
- ¹⁹M. H. MacGregor, R. A. Arndt, and R. M. Wright, Phys. Rev. 182, 1714 (1969).
- ²⁰A. C. Phillips, Nucl. Phys. A107, 209 (1968).
- ²¹L. Mathelitsch, W. Plessas, and W. Schweiger, Phys. Rev. C 26, 65 (1982).
- ²²J. E. Brock, A. Chisholm, J. C. Duder, and R. Garrett, Nucl. Phys. A382, 221 (1982).
- ²³W. Tornow, C. R. Howell, R. C. Byrd, R. S. Pedroni, and R. L. Walter, Phys. Rev. Lett. 49, 312 (1982).